Molecular Biology of the Cell
Vol. 8, 2553–2562, December 1997

Ubiquitously Expressed Dynamin-II Has a Higher Intrinsic GTPase Activity and a Greater Propensity for Self-assembly Than Neuronal Dynamin-I

Dale E. Warnock, Takeshi Baba,* and Sandra L. Schmid†

Department of Cell Biology, The Scripps Research Institute, La Jolla, California 92037

Submitted July 2, 1997; Accepted September 3, 1997
Monitoring Editor: Peter Walter

To begin to understand mechanistic differences in endocytosis in neurons and nonneuronal cells, we have compared the biochemical properties of the ubiquitously expressed dynamin-II isoform with those of neuron-specific dynamin-I. Like dynamin-I, dynamin-II is specifically localized to and highly concentrated in coated pits on the plasma membrane and can assemble in vitro into rings and helical arrays. As expected, the two closely related isoforms share a similar mechanism for GTP hydrolysis: both are stimulated in vitro by self-assembly and by interaction with microtubules or the SH3 domain-containing protein, grb2. Deletion of the C-terminal proline/arginine-rich domain from either isoform abrogates self-assembly and assembly-dependent increases in GTP hydrolysis. However, dynamin-II exhibits a ~threefold higher rate of intrinsic GTP hydrolysis and higher affinity for GTP than dynamin-I. Strikingly, the stimulated GTPase activity of dynamin-II can be >40-fold higher than dynamin-I, due principally to its greater propensity for self-assembly and the increased resistance of assembled dynamin-II to GTP-triggered disassembly. These results are consistent with the hypothesis that self-assembly is a major regulator of dynamin GTPase activity and that the intrinsic rate of GTP hydrolysis reflects a dynamic, GTP-dependent equilibrium of assembly and disassembly.

INTRODUCTION

Dynamin is a 100-kDa GTPase required for late stages in clathrin-mediated endocytosis (Liu and Robinson, 1995; Warnock and Schmid, 1996). A working model for dynamin function has been proposed (Hinshaw and Schmid, 1995) in which the GTPase is first targeted to clathrin-coated pits on the plasma membrane (Damke *et al.*, 1994). GTP binding triggers its release from the clathrin lattice and its self-assembly into helical structures that encircle the necks of deeply invaginated coated pits (Hinshaw and Schmid, 1995; Takei *et al.*, 1995). GTP hydrolysis by dynamin is required for coated vesicle budding (Damke *et al.*, 1994; Herskovits *et al.*, 1993; van der Bliek *et al.*, 1993). Three mammalian isoforms of dynamin have been detected (Liu and Robinson, 1995; Urrutia *et al.*, 1997). The originally identified isoform, now referred to as dynamin-I (dynI), is exclusively expressed in neurons and cells of neuronal lineage (Nakata *et al.*, 1991). Dynamin-II (dynII) is ubiquitously expressed (Cook *et al.*, 1994; Sontag *et al.*, 1994) and dynamin-III (dynIII) is primarily expressed in Sertoli cells of the testis (Nakata *et al.*, 1993, but also see Cook *et al.*, 1996.)

The biochemical properties of dynI have been studied in detail. Isolated dynI self-assembles in vitro in low-salt buffers into ordered formations of rings and helical arrays (Hinshaw and Schmid, 1995), similar morphologically to helical structures assembled at the necks of budding vesicles (Koenig and Ikeda, 1989; Takei *et al.*, 1995). Self-assembly does not require guanine nucleotides but does require the C-terminal proline/arginine-rich domain (PRD) of dynamin (Hinshaw and Schmid, 1995). DynI has a high intrinsic rate of GTP hydrolysis compared with most GTPases, and this activity is further stimulated by a variety of effector molecules, including microtubules, Glutathione *S*-

* Present address: Department of Anatomy, Yamanashi Medical University, Yamanashi 409-38, Japan.
† Corresponding author: Department of Cell Biology, The Scripps Research Institute, 10500 N. Torrey Pines Road, La Jolla, CA 92037.

transferase fusions containing SH3 domains and acidic phospholipids (Gout *et al.*, 1993; Herskovits *et al.*, 1993; Nakata *et al.*, 1991; Shpetner and Vallee, 1992; Tuma *et al.*, 1993). Each of these effectors is multivalent and interacts with dynI through the PRD. The finding that intact monoclonal IgGs directed toward the PRD can also stimulate GTPase activity whereas Fab fragments of the same antibodies cannot suggested that stimulation of dynI GTPase activity required dynamin-dynamin interactions (Warnock *et al.*, 1995). Such a mechanism was also suggested by the observation that both microtubule- and phospholipid-stimulated GTPase activity showed positive cooperativity with respect to dynI concentration (Tuma and Collins, 1994). In fact, dynI self-assembly is itself sufficient to stimulate GTPase activity severalfold (Lin and Gilman, 1996; Warnock *et al.*, 1996). Interestingly, GTP binding triggers disassembly of the supramolecular structures assembled by isolated dynI, and stabilization of assembled dynI molecules by coassembly with mutant dynamin molecules defective in GTP binding greatly enhances the rate of GTP hydrolysis (Warnock *et al.*, 1996). Together these results suggested that GTP hydrolysis in vitro is coupled to a cycle of dynamin assembly and disassembly.

In contrast, the biochemical and functional properties of the ubiquitously expressed dynII isoform have not been studied. Overexpression of dominant-negative mutants of dynI in nonneuronal cells expressing dynII blocks endocytosis (Damke *et al.*, 1994; Herskovits *et al.*, 1993; van der Bliek *et al.*, 1993), whereas other membrane trafficking events are unaffected. Therefore, it has been assumed that dynI and dynII are functionally homologous, although recent reports have suggested that dynII might be localized to the Golgi (Henley and McNiven, 1996; Maier *et al.*, 1996). If dynI and dynII have common functions, why should neuronal and nonneuronal isoforms exist in mammals? Only a single dynamin gene product exists in *Drosophila* (Chen *et al.*, 1991; van der Bliek and Meyerowitz, 1991) and *Caenorhabditis elegans* (Clarke *et al.*, 1997). Moreover, the fact that dynI and dynII share no greater identity between themselves (~70%) than either isoform does with a *shibire* gene from *Drosophila* (Liu and Robinson, 1995; Urrutia *et al.*, 1997; Warnock and Schmid, 1996) suggests that the two isoforms might function differently.

Neuron-specific isoforms exist for many of the proteins involved in the endocytic pathway leading to rapid synaptic vesicle recycling (e.g., clathrin light chains, AP2 complexes, AP180, amphiphysin, etc., reviewed in De Camilli *et al.*, 1995; Morris and Schmid, 1995). Therefore, it is likely that these isoform differences reflect physiological differences between rapid, highly regulated synaptic vesicle retrieval in the neuron and constitutive receptor-mediated endocytosis in nonneuronal cells. To begin to understand how dynamin might differentially function in neuronal and nonneuronal tissues, we have directly compared the biochemical properties of ubiquitously expressed dynII with its better characterized neuron-specific counterpart, dynI. Our results suggest that while the two dynamin isoforms share similar mechanisms of GTP hydrolysis, dynII exhibits significantly greater rates of intrinsic and stimulated GTP hydrolysis than does dynI. Several factors contributed to the enhanced activity of dynII including a higher affinity for GTP, an increased catalytic efficiency, a greater propensity for self-assembly, and enhanced stability of assembled structures.

MATERIALS AND METHODS

Materials

Protease inhibitor cocktail tablets were from Boehringer Mannheim (Indianapolis, IN), and calpain inhibitor I was from Calbiochem (La Jolla, CA). GTP and GDP were from Sigma Chemical Co. (St. Louis, MO). GTPγS and guanylyl-imidodiphosphate were from Boehringer Mannheim. [α-^{32}P]GTP was from Amersham (Arlington Heights, IL). Unless otherwise indicated, all other chemicals were reagent grade.

DynII and Dynamin-ΔPRD Constructs

Rat dynamin-IIa cDNA (from T.C. Südhof, University of Texas Southwestern Medical Center, Dallas, TX) was shuttled into the pVL1393 baculovirus cloning vector and subsequently used to produce high-titer baculovirus stock according to the manufacturer's instructions (PharMingen, La Jolla, CA). ΔPRD dynamin constructs were made with use of the Quikchange PCR mutagenesis kit from Stratagene (La Jolla, CA) to introduce a stop codon at amino acid 751 of dynI and amino acid 747 of dynII. Recombinant baculovirus was prepared as for intact dynII.

Expression of Recombinant Dynamin in Tn5 Cells and Purification of Dynamin Proteins

Dynamins were isolated as previously described (Warnock *et al.*, 1996) with minor modifications. Specifically, dynamins were expressed in recombinant baculovirus-infected Tn5 cells grown in shaking 2-liter baffled flasks (Kontes, Vineland, NJ) at 27°C in ExCel 401 (JRH Biosciences, Lenexa, KS) containing Fungizone (Irvine Scientific, Santa Ana, CA). Cells were infected at 3 to 5 plaque-forming units/cell with high-titer virus stocks and harvested 48 h later by centrifugation at 500 × *g* for 10 min. Homogenization and purification schemes were unchanged, except that chromatography on hydroxyapatite was conducted in buffers without added $CaCl_2$. DynI and dynII, as well as their ΔPRD counterparts, behaved identically during this procedure and yielded up to 15 mg from 2×10^9 infected Tn5 cells. Purity was >95% as judged by Coomassie blue staining after SDS-PAGE. Aliquots were stored at −80°C in 400 mM KPO_4 (pH 7.2) containing 1 mM dithiothreitol (DTT) and 40 μM calpain inhibitor 1.

GTPase Assay

Dynamin was transferred to HEPES column buffer (HCB) containing 150 mM NaCl (HCB150) (HCB is 20 mM HEPES, 2 mM $MgCl_2$, 1 mM EGTA, pH 7.0) or GTPase assay buffer, referred to as PH buffer [20 mM piperazine-*N*,*N*′-bis(2-ethanesulfonic acid)], 20 mM HEPES, 2 mM MgCl, 1 mM EGTA, 1 mM DTT, pH 7.0), by overnight dialysis with two buffer changes. GTPase assays were performed in

PH buffer with 1 mM DTT and 0.1% bovine serum albumin in a final volume of 20 μl, as described (Warnock *et al.*, 1996; Warnock *et al.*, 1995). In all cases, salts were adjusted to maintain a final ionic strength in the assay mixtures of 42 mM because dynamin GTPase activity is sensitive to changes in ionic strength (Tuma *et al.*, 1993; Warnock *et al.*, 1996). K_m and k_{cat} were calculated from Lineweaver-Burk reciprocal plots.

Dynamin Assembly Assays

Dynamin self-assembly into oligomeric structures was assayed as described (Hinshaw and Schmid, 1995) with minor modifications. Dynamins (2 mg/ml in phosphate buffer) were dialyzed into HCB150 for 2 h with two buffer changes, followed by a 10-min centrifugation at 4°C and 14,000 rpm in an Eppendorf 5402 refrigerated microfuge to reduce nonspecific aggregation that occurred during dialysis. Subsequently, protein was diluted 10-fold to a final concentration of 0.2 mg/ml, into either HCB150 (high-salt) or PH (low-salt) buffer on ice. Supernatant and pellet fractions were obtained after centrifugation at 50,000 rpm for 10 min in a TLA100 rotor (Beckman Instruments, Fullerton, CA). Dynamin in each fraction was resolved by SDS-PAGE on 7.5% acrylamide gels. Coomassie brilliant blue-stained gels were quantitated after scanning on a Molecular Dynamics personal densitometer using Molecular Dynamics ImageQuant software as described previously (Warnock *et al.*, 1996). Alternatively, light scattering at A_{320} of dynamin upon assembly was measured at ambient temperature to follow the progression over time or at equilibrium. 1.0- or 0.4-cm cuvettes were used for measurements, with final values converted to a 1.0-cm path length. These measurements were made with a Beckman DU-100 spectrophotometer.

Preparation of "Ripped-Off" Plasma Membranes from A431 Cells and Immunogold Localization of Endogenous DynII

Perforated A431 cells were incubated for 30 min at 37°C in the presence of human K562 erythroleukemic cell cytosol, an ATP-regenerating system, and 100 μM GTP, GTPγS, or GDPβS as previously described (Carter *et al.*, 1993). The perforated cells were returned to ice and then pelleted onto poly-L-lysine-coated coverslips. Electron microscopy (EM) grids were applied to the upper surface of the cells. These were subsequently removed carrying large areas of the plasma membrane onto the EM grids as described (Sanan and Anderson, 1991). These "ripped-off" plasma membranes preparations were then fixed (4% paraformaldehyde, 1% glutaraldehyde) and immuno-stained for dynamin using hudy-1 mAb (Warnock *et al.*, 1995) and 10-nm gold-conjugated secondary antibodies (Ted Pella, Redding, CA). Immunogold-labeled membranes were then fixed with 4% glutaraldehyde and stained for clathrin lattices as previously described (Damke *et al.*, 1994). EM negatives were scanned at 400 pixels/in using a Umax Model UC1260 scanner. Negatives were coded and quantitation was performed with NIH Image Software. The assignment of experimental conditions was made only after analysis.

For negative stain images, dynamins (2.5 mg/ml) were dialyzed overnight in HCB30 plus 1% ethylene glycol, 0.5 mM DTT. Samples were then diluted to 0.25 mg/ml into HCB30 and applied to EM grids. Alternatively, dynamins (0.1 mg/ml final concentrations) were added to preassembled, taxol-stabilized microtubules (0.1 mg/ml) in PH buffer and bound to EM grids for 3 min. Grids were washed briefly, negatively stained in 2% uranyl acetate for 3 min, and examined under a Philips CM10 electron microscope (Philips Technologies, Cheshire, CT). The negatives were recorded at 35,500×. The images were then scanned using a LeafScan 45 scanner at 20 pixels/mm.

RESULTS

Guanine Nucleotides Affect DynII Localization on Plasma Membrane-associated Clathrin-coated Pits

Although it has been assumed that dynI and dynII have similar functions, albeit in different tissues, no direct evidence was available for the role of dynII in endocytic clathrin-coated vesicle formation. The possibility has even been raised, based on immunolocalization and subcellular fractionation (Henley and McNiven, 1996; Maier *et al.*, 1996), that dynII might function at the Golgi. Immunofluorescence experiments with the antidynamin monoclonal antibody, hudy-1 showed punctate plasma membrane-associated staining. As we reported for HeLa cells expressing endogenous dynII (Damke *et al.*, 1994), aside from a diffuse cytosolic staining, there was no detectable label in the perinuclear region in A431 cells (unpublished results). Immunogold labeling on isolated "ripped-off" plasma membrane preparations showed that dynII was highly concentrated in coated pits on the plasma membrane (Figure 1). Quantitative analysis revealed that 89% of gold particles (4497 of 5036 counted) were associated with clathrin-coated pits (morphologically distinguished by their characteristic polygonal lattice), even though these structures represented <1% of total surface area measured (1.72-μm^2 coated pits/292.8-μm^2 plasma membrane). The average number of gold particles per coated pit was 14 ± 7 (range, 1–40). This represents an ~140-fold enrichment of plasma membrane-associated dynII in coated pits.

Two predominant patterns of localization relative to coated pits were observed. DynII was detected randomly distributed over clathrin lattices on flat or curved coated pits (Figure 1, a–c). This distribution was similar to that seen in HeLa cells overexpressing the K44A mutant of dynI defective in GTP binding and hydrolysis (Damke *et al.*, 1994). A second distinct pattern of dynamin localization was observed on more deeply invaginated coated pits. In these structures, often demarcated by an electron-dense "puddle" of stain encircling the necks at their base, labeling appeared to be segregated from the clathrin lattice and to encircle the pit (Figure 1, d–f). This distribution corresponded more closely to that observed on presynaptic membranes of *shibire* flies incubated at the nonpermissive temperature (Koenig and Ikeda, 1989) or in permeabilized rat synaptosomal membranes treated with GTPγS (Takei *et al.*, 1995). Under these conditions, dynI is seen to assemble into electron-dense collars around the necks of invaginated coated pits that are spatially resolved from the clathrin coat remaining on the bud. Thus, the two patterns seen suggested that like dynI, dynII undergoes a redistribution relative to the clathrin lattice during coated vesicle budding.

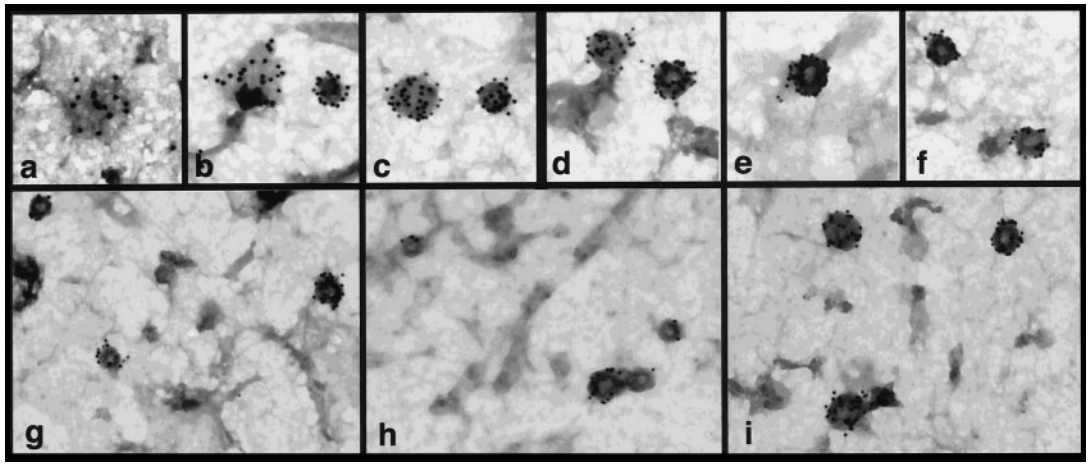

Figure 1. Guanine nucleotides influence the distribution of dynII on coated pits in A431 cells. Upper panels show coated pits with various degrees of curvature detected at steady state on ripped-off plasma membrane preparations from perforated A431 cells. Endogenous dynII was detected using hudy-1 mAb followed by 10 nm gold-conjugated secondary antibodies. Dynamin is uniformly distributed on flat lattices (a, b) and on curved coated pits (b–d) but is localized peripherally at the base around the more deeply invaginated coated pits (e, f) distinguished by the pool of stain encircling their base. Lower panels show representative fields from perforated A431 cells incubated in the presence of GTP (g), GTPγS (h), or GDPβS (i). ~39,000×.

Interestingly, the relative distribution of dynII between these two localizations in perforated A431 cells could be affected by incubation with guanine nucleotide analogues. When perforated cells were incubated with cytosol derived from human K562 erythroleukemic cells (which also express only dynII) in the presence of either GTP (Figure 1g) or the nonhydrolyzable analogue GTPγS (Figure 1h), 60% (n = 118) and 58% (n = 158) of coated pits examined exhibited peripheral dynamin labeling at their base and a depletion of dynamin label from the clathrin lattice. In contrast, when incubations were performed in the presence of GDPβS (Figure 1i), the proportion of lattices exhibiting peripheral dynII labeling significantly decreased to 10% while uniform lattice labeling by dynII increased to 90% (n = 182). These results suggest that guanine nucleotides regulate the interactions of dynII with coated pits in a manner similar to their effects on dynI.

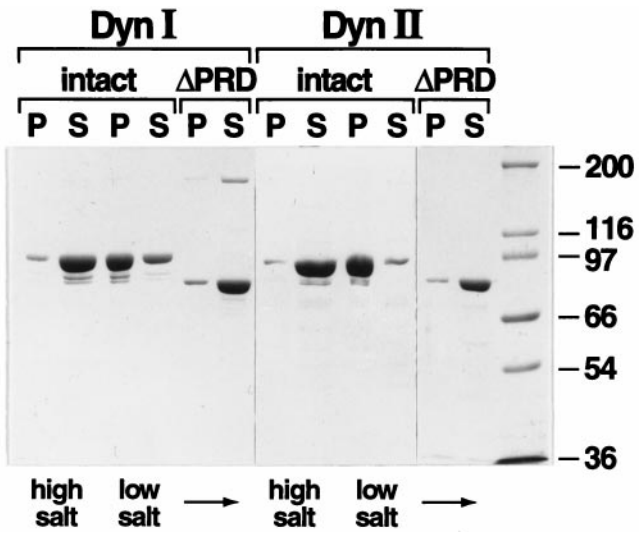

Figure 2. Self-assembly of dynI and dynII is dependent on an intact PRD. Self-assembly of dynI and dynII and their ΔPRD counterparts was followed by a sedimentation assay that separates dynamin structures that pellet (P) from unassembled dynamin that remains in the supernatant (S) after centrifugation at 100,000 × *g* for 15 min. Dynamins (in HCB150) were diluted 10-fold to a final protein concentration of 0.2 mg/ml, into either HCB150 (high-salt) or PH (low-salt) buffer. Equal aliquots of soluble and pelleted dynamin were analyzed by SDS-PAGE on 7.5% acrylamide gels and detected by Coomassie brilliant blue staining. The full gels are shown to demonstrate the purity of the protein preparation. Molecular weight protein standards are as indicated.

DynII Self-Assembles into Rings and Helical Stacks of Rings

The accumulated evidence suggests that dynII functions like dynI in endocytic coated vesicle formation. To determine what biochemical properties of the two isoforms might be contributing to their tissue-specific functions the biochemical properties of the ubiquitously expressed isoform dynII were compared with those of the previously characterized neuronal isoform dynI. Both proteins were expressed and purified from recombinant baculovirus-infected Tn5 cells to exclude possible effects of tissue-specific posttranslational modifications. After dilution into low-ionic-strength buffers, dynI self-assembles into sediment-

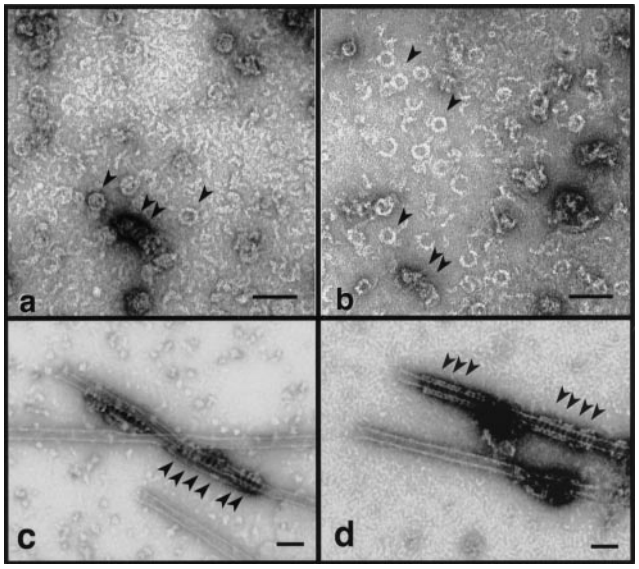

Figure 3. DynI and dynII self-assemble into similar oligomeric structures. DynI (a) and dynII (b) were self-assembled by dialysis into HCB30 containing 1% ethylene glycol and examined by electron microscopy in negative stain. Arrowheads indicate rings and small stacks of rings. In c and d, dynI and dynII, respectively, were incubated with taxol-stabilized microtubules at 0.1 mg/ml in PH buffer. Final dynamin concentration in each condition was 0.1 mg/ml. Arrowheads show dynamin rings encircling the microtubule template. Bars, 100 nm.

able structures (Figure 2) that resemble rings and small helical stacks of rings as viewed by negative stain electron microscopy (Figure 3a). Because these structures are similar to electron-dense "collars" captured around the necks of invaginating coated pits in *shibire* flies (Koenig and Ikeda, 1989), we have speculated that dynamin self-assembly is essential for its function in vivo. To gain some insight into whether dynII might function similarly in vesicle budding, we tested whether dynII could self-assemble into similar structures. Like dynI, short 10-nm-thick rods and extended strands of dynII were prevalent at higher salt concentrations (unpublished results). Upon dilution or dialysis into low-salt buffers, dynII assembled into sedimentable structures (Figure 2) that resembled closed rings (~40 nm in diameter) and small stacks of rings (Figure 3b, arrowheads) similar to those seen with dynI. At higher concentrations, dynI formed long, uniform spirals upon dialysis into low-ionic-strength conditions (Hinshaw and Schmid, 1995). In contrast, under these conditions, dynII had a much greater tendency to form large knots of greatly extended linear strands of protein (unpublished results). However, when provided with a uniform template, such as microtubules, both isoforms assembled into helical arrays of similar dimension (Figure 3, c and d, arrowheads).

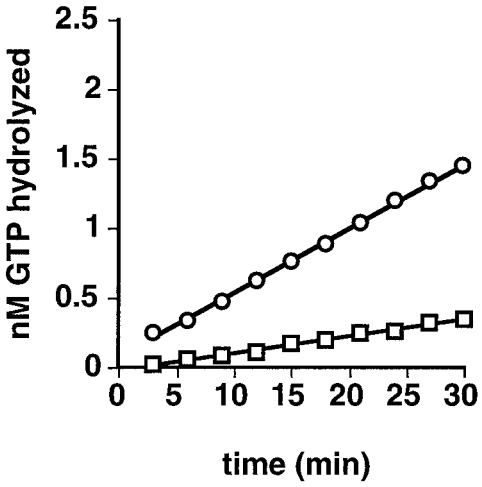

Figure 4. DynII has a higher endogenous rate of GTP hydrolysis than dynI. Intrinsic GTPase activities of dynI (□) and dynII (○) were measured in 20 μl of PH buffer as described in EXPERIMENTAL PROCEDURES and containing 0.2 μg of dynamin and 0.25 mM GTP. Backgrounds obtained without dynamin have been subtracted. A representative experiment is shown; average rates determined from four independent experiments are given in the text.

Intrinsic DynII GTPase Activity Displayed Positive Cooperative Behavior

We next compared the GTPase activity of the two dynamin isoforms. The data in Figure 4 show that the intrinsic GTPase activity of dynII, measured at 0.1 μM, was significantly higher (10.7 ± 3.3-fold, n = 4) than that of dynI. Like dynI, dynII GTPase activity could be further stimulated by microtubules, and a glutathione *S*-transferase fusion of the SH3 domain-containing protein grb2 (our unpublished results).

We previously showed that the intrinsic GTPase activity of dynI is highly cooperative and that dynamin self-assembly potently stimulates the rate of GTP hydrolysis (Warnock *et al.*, 1996). Thus, the higher intrinsic GTPase activity of dynII compared with dynI could reflect a greater propensity for dynII to self-assemble. To test this possibility, we compared the positive cooperative behavior of dynII GTPase activity with that of dynI by measuring the rates of GTP hydrolysis in the presence of increasing concentrations of dynamin. As previously reported, the specific activity of dynI GTPase increased sharply from a basal rate of ~2 min^{-1} at low concentrations of dynI to reach a maximum of ~8 min^{-1} at dynamin concentrations exceeding 1 μM (Figure 5B). DynII also showed strong positive cooperativity; however, there was a much sharper concentration-dependent increase in specific activity, reaching a maximum of ~80 min^{-1} at 0.5 μM dynII (Figure 5A). At 0.5 μM dynamin, the intrinsic GTPase rate of dynII was on average 50-fold (53.8 ± 22, n = 4) greater than that of dynI.

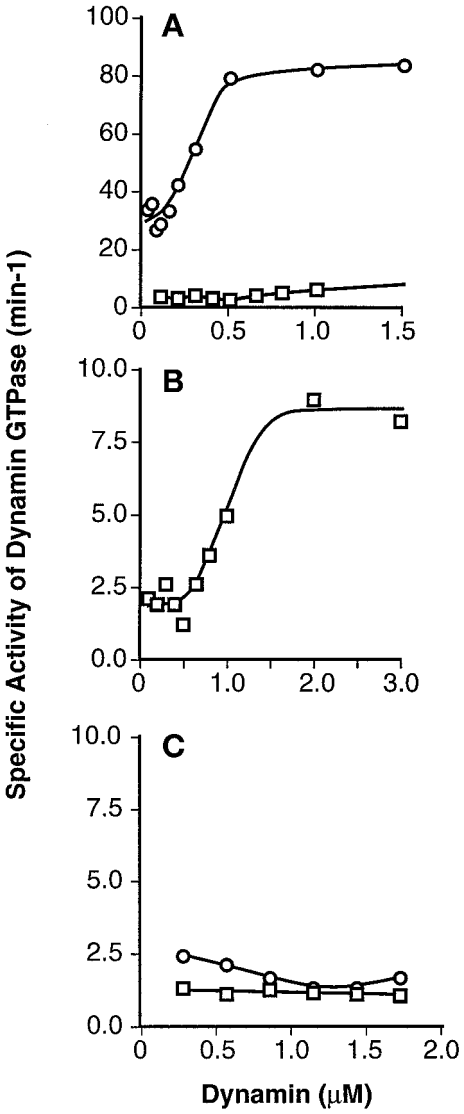

Figure 5. The positive cooperative behavior of dynII GTPase activity requires the C-terminal PRD. GTPase activities of increasing dynamin concentrations were measured as described in EXPERIMENTAL PROCEDURES. (A) Concentration dependence of the specific activity of dynII as compared with dynI. Data for dynI are replotted on an expanded scale in B to illustrate the cooperative behavior of dynI specific activity. C compares the specific activities of truncated dynI and dynII, lacking their C-terminal PRD. Each point represents the linear rate of GTP hydrolysis derived from five time points. Data are representative of three separate experiments.

The C-terminal PRD Is Required for the Cooperative Behavior of Dynamin GTPase

Previous studies had shown that truncated forms of dynI in which the PRD had been cleaved by limited proteolysis exhibited unimpaired intrinsic GTPase activity but no longer exhibited microtubule-, grb2-, or phospholipid-stimulated GTPase activity (Herskovits *et al.*, 1993; Tuma *et al.*, 1993). Limited C-terminal proteolysis of dynamin also abrogates its ability to self-assemble (Hinshaw and Schmid, 1995). The C termini of the digestion products of limited proteolysis were variable and difficult to define; therefore, we constructed C-terminal PRD deletion mutants of both dynamin isoforms by inserting premature stop codons after residue 751 of dynI and residue 747 of dynII, resulting in deletion of the C-terminal 111 and 122 residues, respectively. As expected, although both intact dynamin isoforms self-assemble into sedimentable structures upon dilution into low-ionic-strength buffers, neither ΔPRD isoform exhibited appreciable self-assembly activity (Figure 2).

The GTPase activity of both ΔPRD isoforms is shown in Figure 5C. Consistent with our previous hypothesis that the cooperative behavior of dynI GTPase activity reflected its self-assembly properties, cooperativity was abrogated in the ΔPRD-dynI mutant. The basal rate of GTP hydrolysis (1.01 ± 0.38 min^{-1}, n = 24) was unaffected by ΔPRD-dynI concentration (0.25–1.5 μM dynamin). Similarly, the positive cooperative behavior of dynII GTPase activity was lost in the ΔPRD-dynII mutant. Instead, we observed a small but reproducible decrease in the basal rate for GTP hydrolysis from 4.83 ± 1.11 min^{-1} (n = 4) at 0.25 μM dynamin to 2.17 ± 0.63 min^{-1} at >0.75 μM dynamin. Importantly, compared with the large differences seen between intact dynamin isoforms, the specific GTPase activities of ΔPRD isoforms were similar. These data suggested that the ~50-fold differences in specific intrinsic GTPase activity between dynI and dynII were largely attributable to differences in self-assembly properties of the two isoforms.

DynII Has a Higher Propensity for Self-assembly Than DynI

The GTPase activity of ΔPRD-dynII was significantly less than that for intact dynII even when the latter was measured under dilute protein concentrations (compare Figure 5A with Figure 5C). By contrast, the specific activity of ΔPRD-dynI was comparable with that of intact dynI measured at low protein concentrations (compare Figure 5B with Figure 5C). These results suggested that intact dynII has a greater propensity for self-association at low concentrations than does dynI. To test this directly, we compared the self-association characteristics of the two dynamin isoforms quantitatively by measuring increases in light scattering due to dynamin self-assembly into higher order structures (Figure 6). Whereas sedimentation of dynamin provides qualitative data on the formation of large oligomers, light scattering measurements are sensitive to the size of oligomers and amenable to kinetic analysis. A similar approach has been used by others to measure clathrin assembly (Crowther and Pearse, 1981; Liu *et al.*, 1995). Control experiments

established that increases in absorbance at 320 nm correlated with dynamin self-assembly as measured by sedimentation. Specifically, there was no increase in light scattering either when dynamin was maintained in high-salt buffers or with either ΔPRD-dynI or ΔPRD-dynII even at low ionic strength (unpublished results). To compare the concentration dependence for self-assembly of dynI and dynII, we diluted stock solutions of each isoform in HCB150 10-fold into cuvettes containing salt-adjusted buffer to give the indicated final concentrations of dynamin in PH buffer. DynII self-assembly was detected even at low concentrations of protein, while dynI self-assembly required much higher concentrations and showed greater cooperativity (Figure 6A).

Dynamin GTPase Activity Reflects a Dynamic Equilibrium between Assembled and Unassembled States

We previously showed that the GTP concentration used in our assays triggers the disassembly of assembled dynI and that stabilization of assembled dynI against GTP-induced disassembly significantly stimulates its specific GTPase activity (Hinshaw and Schmid, 1995; Warnock *et al.*, 1996). These observations led us to propose that the GTPase activity of dynamin in vitro reflects a dynamic equilibrium between assembly and disassembly. Like dynI, dynII assembly is also affected by GTP. Figure 6b shows that when the dynamin isoforms are diluted into low-ionic-strength buffers containing 250 μM GTP, the extent of assembly at steady state was greatly reduced (compare Figure 6A with Figure 6B). In fact, dynI assembly as measured by light scattering was not apparent. This suggests that either dynI assembly under these conditions was transient or that smaller structures were formed, or both. As was observed in the absence of GTP, dynII assembled to a greater extent and at lower concentrations than dynI in the presence of GTP. The nonhydrolyzable analogue guanylyl-imidodiphosphate even more potently impaired stable self-assembly of dynI and dynII, whereas GDP had no effect at these concentrations (<250 μM) (unpublished results). Thus, the higher GTPase activity correlates well with the enhanced propensity of dynII for self-assembly and with the increased stability of assembled dynII in the presence of GTP.

DynII Has a Higher Affinity for GTP Than DynI

We next sought to compare the kinetic parameters of GTPase activity for the two dynamin isoforms. However, these experiments are complicated by the fact that dynI and dynII differ in their propensity for self-assembly, and we have shown that the assembly state of dynamin affects the behavior of GTPase activity (Warnock *et al.*, 1996). Therefore, to measure the kinetic parameters of GTPase activity independent of differences in self-assembly properties, we first analyzed the ΔPRD truncation mutants of the two isoforms. The data in Figure 7A show Michaelis-Menten kinetic behavior of dynI and dynII measured by Lineweaver-Burk reciprocal plot analysis. ΔPRD-dynII exhibited a 3.5-fold greater k_{cat} (2.8 min^{-1}) and a threefold lower K_m for GTP (12 μM) than did ΔPRD-dynI (0.8 min^{-1} and 36 μM, respectively). To compare kinetic parameters for assembly-stimulated GTPase activity under conditions where differences in their propensity for self-assembly would be minimized, we took advantage of the fact that microtubules provide a

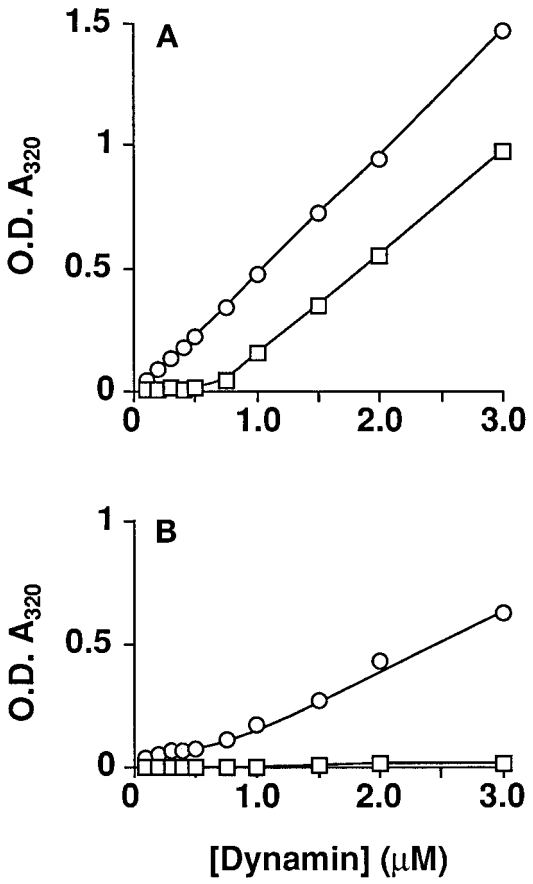

Figure 6. DynII shows a greater propensity for self-assembly than dynI. Light scattering measured at $A_{320\ nm}$ was used to follow dynamin self-assembly as described in EXPERIMENTAL PROCEDURES. DynI (□) or dynII (○) at 2 mg/ml in HCB150 was diluted to the indicated protein concentrations in PH buffer in the absence (A) or presence (B) of 250 μM GTP. Assays were in a final volume of 200 μl of PH buffer, fixed at 50 mM ionic strength. Steady-state assembly was reached after 20 min even at low protein concentrations, at which point the absorbance values shown were recorded. Care was taken at higher protein concentrations that readings of light scattering were taken well before complete hydrolysis of the GTP. Each point represents the mean derived from three independent determinations with all standard deviations smaller than the symbols. Data are representative of three separate experiments.

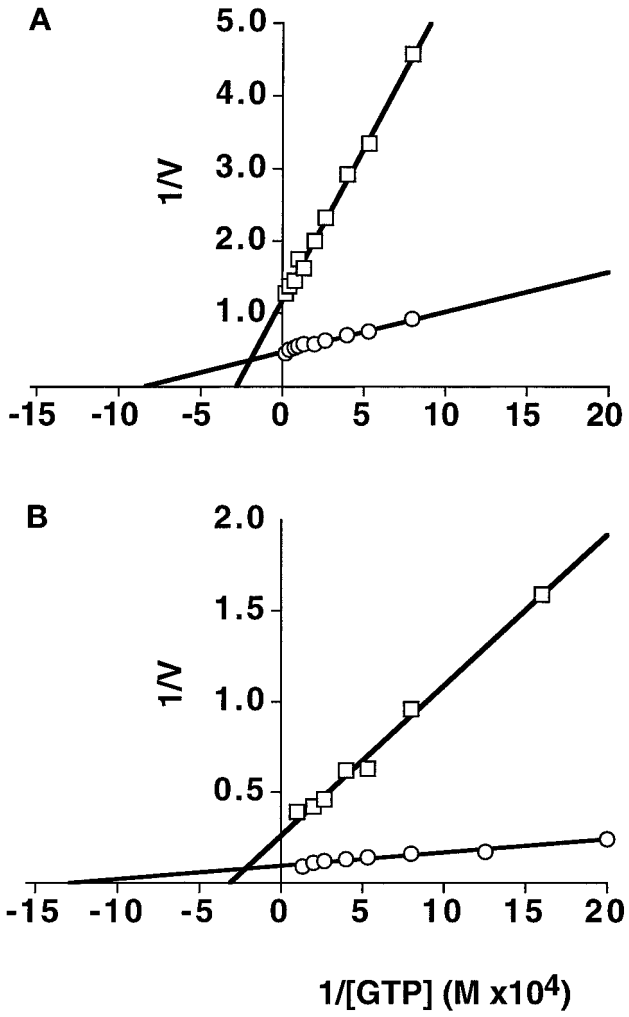

Figure 7. Michaelis-Menton kinetics of GTP hydrolysis by dynI and dynII. The assembly-independent rates of GTP hydrolysis (A) were determined using ΔPRD mutants of dynI (□) and dynII (○) (at 1.3 μM and 0.88 μM, respectively) in the presence of increasing concentrations of GTP and a plot of $1/V$ (nmol/l/min) versus 1/[GTP] (M) is shown. Assembly-dependent rates of GTP hydrolysis (B) were determined for dynI (□) and dynII (○) (both at 0.1 μM) in the presence of 0.1 mg/ml taxol-stabilized microtubules.

template for, and stabilize the cooperative assembly of, both dynI and dynII (Figure 3, c and d). Microtubules stimulated GTPase activities of both isoforms by ~40-fold over the activity of ΔPRD-dynamins. The data in Figure 7B show that the microtubule-stimulated rate of GTP hydrolysis of dynII (k_{cat} = 109.7 min^{-1}) was again ~threefold greater than that of dynI (k_{cat} = 38.6 min^{-1}). Microtubule interactions appeared not to significantly affect the K_m for GTP of either isoform (K_m = 13 μM for dynII and 32 μM for dynI in the presence of microtubules). Together, these data suggest that dynII has greater intrinsic catalytic activity than dynI, independent of its greater propensity for self-assembly.

DISCUSSION

Considerable evidence supports a role for dynI in endocytosis (Urrutia *et al.*, 1997; Warnock and Schmid, 1996); however, direct evidence for the function of dynII has been lacking. The localization and high degree of concentration of endogenous dynamin at coated pits on the plasma membrane of A431 cells are most consistent with a similar role for dynII, specifically in endocytic vesicle formation in nonneuronal cells. The mAb we have used for this study, hudy-1, specifically recognizes an epitope in the PRD of dynI and dynII that is not conserved among other more distantly related dynamin family members (Warnock *et al.*, 1995). A previous study using antipeptide antibodies directed toward highly conserved epitopes in the GTPase domain (Henley and McNiven, 1996) had suggested that dynII might be localized to *cis* and/or medial cisternal elements of the Golgi (labeling was not detected in the *trans*-Golgi network). It remains a possibility that these antibodies were detecting an as yet unidentified dynamin family member, perhaps more closely related to Vps1p, a GTPase that functions in Golgi-vacuolar trafficking in yeast (Rothman *et al.*, 1990).

DynII exhibited two distinct guanine nucleotide-sensitive distributions relative to the clathrin lattice. In perforated A431 cells incubated with GDPβS, dynII accumulated in a diffuse distribution throughout the clathrin lattice, whereas in cells incubated with GTP or GTPγS, dynII was peripherally distributed around the base of the majority of coated pits. This finding supports the model, based on previous studies with dynI, that GTP binding is required to trigger the redistribution and assembly of dynamin at the necks of deeply invaginated coated pits. That dynamin was similarly distributed after incubation with either GTP or GTPγS was consistent with previous studies showing that constricted coated pits accumulate in perforated cells incubated under these conditions (Carter *et al.*, 1993).

Interestingly, although dynamin collars are apparent on the endocytic buds that accumulate on the presynaptic membrane in *Drosophila* expressing the *shibire* mutation, they have not been detected in nonneuronal tissues, even though coated buds accumulate on the plasma membrane (Koenig and Ikeda, 1989; Koenig and Ikeda, 1990; reviewed in Warnock and Schmid, 1996). Therefore, it was possible that these structures were specific to the neuron and perhaps to neuronal isoforms of dynamin. The simple EM technique we have used is insufficient to detect dynamin collars, such as those detected by thin-section analysis of permeabilized synaptosomes treated with GTPγS (Takei *et al.*, 1995). However, at low ionic strength,

dynII formed rings and small stacks of rings similar in dimension to the dynI collars detected at the synapse. Unambiguous identification of dynII function and identification of dynII collars in vivo will require detailed biochemical and morphological analysis of stable cell lines expressing dominant-negative mutants of dynII that block coated vesicle formation at discrete stages. Interestingly, inhibition of endocytosis in transformed HeLa cells requires >10-fold overexpression of dominant-negative dynI mutants, presumably for effective interference with endogenous dynII function (Damke *et al.*, 1994). By contrast, in *Drosophila* that express only a single dynamin isoform, hemizygous *shibire* mutants show strong defects in endocytosis (Kim and Wu, 1990). It is possible, given their relative affinities for self-assembly, that dominant-negative mutants of dynI are less potent inhibitors of dynII function than would be the homologous dynII mutants.

Our results establish, perhaps not unexpectedly, that the two closely related dynamin isoforms share a similar mechanism for GTP hydrolysis: both are stimulated in vitro by self-assembly at higher concentrations of protein or at lower protein concentrations in the presence of either grb2 or microtubules. However, dynII exhibits a significantly higher rate of GTP hydrolysis than dynI due to several contributing factors: 1) its K_m for GTP hydrolysis is ~threefold lower than that for dynI; 2) both the assembly-independent k_{cat} for GTP hydrolysis as measured using the ΔPRD mutants and the maximal stimulated rate of GTP hydrolysis measured in the presence of microtubules are ~threefold greater for dynII than for dynI. However, the most significant contributing factors to the higher rate of GTP hydrolysis observed with intact dynII are its greater propensity for self-assembly and the increased stability of assembled dynII in the presence of GTP. These properties were reflected in the highly cooperative behavior of dynII and the 40- to 50-fold increase in specific GTPase activity of isolated dynII over dynI measured under self-assembly conditions.

The GTPase characteristics of dynII strongly support a model in which dynamin self-assembly is the major regulator of GTPase activity (Tuma and Collins, 1994; Warnock *et al.*, 1996; Warnock *et al.*, 1995). They further suggest that the rate of GTP hydrolysis by dynamin in vitro reflects a dynamic equilibrium between assembled and unassembled molecules. Because the PRD is required for dynamin self-assembly, we speculate that each of the multivalent effectors that stimulate GTP hydrolysis through interactions with the PRD do so by shifting this dynamic equilibrium toward the assembled state. Some effectors, such as microtubules and acidic phospholipid vesicles, might enhance dynamin assembly by providing a uniform template for assembly. Microtubules, for example, have the same dimensions as the narrow membranous necks encircled by dynamin collars in vivo and may therefore mimic this geometry. Other effectors, such as bifunctional mAbs or grb2, might act by cross-linking and stabilizing self-assembled structures.

The ΔPRD mutants did not exhibit positive cooperativity, indicating that the basal rate of GTP hydrolysis does not require intermolecular collisions. However, dynamin-dynamin interactions can stimulate GTP hydrolysis by >40-fold. It will be important to identify which region(s) in dynamin is important for self-assembly, for stability of the assembled complex, and for the intermolecular stimulation of GTPase activity. In this regard, our finding that the closely related isoforms dynI and dynII exhibit biochemically distinct properties suggest that dynI/dynII chimeric molecules might help to identify these functional domains. Identification of these domains is a prerequisite to understanding the mechanism of dynamin stimulated GTP hydrolysis.

Finally, what might be the functional significance of the two dynamin isoforms? The lower affinity for dynI-dynI interactions may prevent unregulated self-assembly at the synapse where it is present at high concentrations. Our estimates, by Western blot analysis, indicate that dynamin is expressed at >100-fold higher levels (per milligram of protein) in rat brain lysates than in lysates from nonneuronal rat tissues (L. Terlecky, D.E.W., and S.L.S., unpublished results). It seems paradoxical, however, that the neuronal isoform required for rapid endocytosis should hydrolyze GTP more slowly than the nonneuronal isoform. However, dynamin GTPase activity appears not to be rate limiting for endocytosis in nonneuronal cells given that >10-fold overexpression of the slower dynI isoform has no effect on receptor-mediated endocytosis (Damke *et al.*, 1994). We speculate, therefore, that the slower rate of GTP hydrolysis and the lower propensity for self-assembly by dynI provides an opportunity for tighter regulation of the activity of this isoform. For example, the neuron-specific phosphorylation of dynI by protein kinase C is reported to stimulate its GTPase activity ~10-fold (Robinson *et al.*, 1993). DynII appears not to be a substrate for protein kinase C phosphorylation (Sontag *et al.*, 1994). Greater insight into the physiological significance of the differing enzymological properties of these isoforms requires further understanding of dynamin function in both neuronal and nonneuronal cells.

ACKNOWLEDGMENTS

We thank Amy Muhlberg, Sanya Sever, Frances Brodsky, and Joel Ybe for helpful discussions. John Elder (the Scripps Research Institute) helped with Tn5 cells and baculovirus expression. Mike McCaffery (University of California at San Diego), Mike Whittacker (the Scripps Research Institute), and Jenny Hinshaw (National Institutes of Health) helped with electron microscopy. EM facilities were provided by the ImmunoEM core funded by National Cancer

Institute Program Project grant CA58689. This work was supported by National Institutes of Health grant GM42455 to S.L.S. S.L.S. is an Established Investigator of the American Heart Association. D.E.W. was supported by American Heart Association Postdoctoral Fellowship 95-142. This is the Scripps Research Institute manuscript number 10819-CB.

REFERENCES

Carter, L.L., Redelmeier, T.E., Woollenweber, L.A., and Schmid, S.L. (1993). Multiple GTP-binding proteins participate in clathrin-coated vesicle-mediate endocytosis. J. Cell Biol. *120*, 37–45.

Chen, M.S., Ober, R.A., Schroeder, C.C., Austin, T.W., Poodry, C.A., Wadsworth, S.C., and Vallee, R.B. (1991). Multiple forms of dynamin are encoded by *shibire*, a *Drosophila* gene involved in endocytosis. Nature *351*, 583–586.

Clark, S.G., Shurland, D.-L., Meyerowitz, E.M., Bargmann, C.I., and van der Bliek, A.M. (1997). A dynamin GTPase mutation causes a rapid reversible temperature-inducible locomotion defect in *C. elegans.* Proc. Natl. Acad. Sci. USA *94*, 10438–10443.

Cook, T., Mesa, K., and Urrutia, R. (1996). Three dynamin encoding genes are differentially expressed in developing rat brain. J. Neurochem. *67*, 927–931.

Cook, T.A., Urrutia, R., and McNiven, M.A. (1994). Identification of dynamin 2, an isoform ubiquitously expressed in rat tissues. Proc. Natl. Acad. Sci. USA *91*, 644–648.

Crowther, R.A., and Pearse, B.M., F. (1981). Assembly and packing of clathrin into coats. J. Cell Biol. *91*, 790–797.

Damke, H., Warnock, D.E., Baba, T., and Schmid, S.L. (1994). Induction of mutant dynamin specifically blocks endocytic coated vesicle formation. J. Cell Biol. *127*, 915–934.

De Camilli, P., Takei, K., and McPherson, P.S. (1995). The function of dynamin in endocytosis. Curr. Opin. Neurobiol. *5*, 559–565.

Gout, I., Dhand, R., Hiles, I.D., Fry, M.J., Panayotou, G., Das, P., Truong, O., Totty, N.F., Hsuan, J., Booker, G.W., Campbell, I.D., and Waterfield, M.D. (1993). The GTPase dynamin binds to and is activated by a subset of SH3 domains. Cell *75*, 25–36.

Henley, J.R., and McNiven, M.A. (1996). Association of a dynamin-like protein with the Golgi apparatus in mammalian cells. J. Cell Biol. *133*, 761–775.

Herskovits, J.S., Burgess, C.C., Ober, R.A., and Vallee, R.B. (1993). Effects of mutant dynamin on endocytosis. J. Cell Biol. *122*, 565–578.

Herskovits, J.S., Shpetner, H.S., Burgess, C.C., and Vallee, R.B. (1993). Microtubules and Src homology 3 domains stimulate the dynamin GTPase via its C-terminal domain. Proc. Natl. Acad. Sci. USA *90*, 11468–11472.

Hinshaw, J.E., and Schmid, S.L. (1995). Dynamin self-assembles into rings suggesting a mechanism for coated vesicle budding. Nature *374*, 190–192.

Kim, Y.-T., and C.-Wu, F. (1990). Allelic interaction at the *shibire* locus of *Drosophila*: effects on behavior. J. Neurogenet. *7*, 1–14.

Koenig, J.H., and Ikeda, K. (1989). Disappearance and reformation of synaptic vesicle membrane upon transmitter release observed under reversible blockage of membrane retrieval. J. Neurosci. *9*, 3844–3860.

Koenig, J.H., and Ikeda, K. (1990). Transformational process of the endosomal compartment in nephrocytes of *Drosophila melanogaster*. Cell Tissue Res. *262*, 233–244.

Lin, H.C., and Gilman, A.G. (1996). Regulation of dynamin 1 GTPase activity by G protein $\beta\gamma$ subunits and phosphatidylinositol 4,5-bisphosphate. J. Biol. Chem. *271*, 27979–27982.

Liu, J.-P., and Robinson, P.J. (1995). Dynamin and endocytosis. Endocrine Rev, *16*, 590–607.

Liu, S.-H., Wong, M.L., Craik, C.S., and Brodsky, F.M. (1995). Regulation of clathrin assembly and trimerization defined using recombinant triskelion hubs. Cell *83*, 257–267.

Maier, O., Knoblish, M., and Westermann, P. (1996). Dynamin-II binds to the trans-Golgi network. Biochem. Biophys. Res. Commun. *223*, 229–233.

Morris, S.A., and Schmid, S.L. (1995). Synaptic vesicle recycling: the Ferrari of endocytosis? Curr. Biol. *5*, 113–115.

Nakata, T., Iwamoto, A., Noda, Y., Takemura, R., Yoshikura, H., and Hirokawa, N. (1991). Predominant and developmentally regulated expression of dynamin in neurons. Neuron *7*, 461–469.

Nakata, T., Takemura, R., and Hirokawa, N. (1993). A novel member of the dynamin family of GTP-binding protein is expressed specifically in the testes. J. Cell Sci. *105*, 1–5.

Robinson, P.J., Sontag, J.-M., Liu, J.P., Fykse, E.M., Slaughter, C., McMahon, H., and Südhof, T.C. (1993). Dynamin GTPase regulated by protein kinase C phosphorylation in nerve terminals. Nature *365*, 163–166.

Rothman, J.H., Raymond, C.K., Gilbert, T., O'Hara, P.J., and Stevens, T.H. (1990). A putative GTP binding protein homologous to interferon-inducible Mx proteins performs an essential function in yeast protein sorting. Cell *61*, 1063–1074.

Sanan, D.A., and Anderson, R.G.W. (1991). Simultaneous visualization of LDL receptor distribution and clathrin lattices on membranes torn from the upper surface of cultured cells. J. Histochem. Cytochem. *39*, 1017–1024.

Shpetner, H.S., and Vallee, R.B. (1992). Dynamin is a GTPase stimulated to high levels of activity by microtubules. Nature *355*, 733–735.

Sontag, J.-M., Fykse, E.M., Ushkaryov, Y., Liu, J.-P., Robinson, P.J., and T.C. Südhof. (1994). Differential expression and regulation of multiple dynamins. J. Biol. Chem. *269*, 4547–4554.

Takei, K., McPherson, P., Schmid, S.L., and De Camilli, P. (1995). Tubular membrane invaginations coated by dynamin rings are induced by GTPγS in nerve terminals. Nature *374*, 186–190.

Tuma, P.L., and Collins, C.A. (1994). Activation of dynamin GTPase is a result of positive cooperativity. J. Biol. Chem. *269*, 30842–30847.

Tuma, P.L., Stachniak, M.C., and Collins, C.A. (1993). Activation of dynamin GTPase by acidic phospholipids and endogenous rat brain vesicles. J. Biol. Chem. *268*, 17240–17246.

Urrutia, R., Henley, J.R., Cook, T., and McNiven, M.A. (1997). The dynamins: redundant or distinct functions for an expanding family of related GTPases? Proc. Natl. Acad. Sci. USA *94*, 377–384.

van der Bliek, A. M., and Meyerowitz, E.M. 1991. Dynamin-like protein encoded by the *Drosophila shibire* gene associated with vesicular traffic. Nature *351*, 411–414.

van der Bliek, A.M., Redelmeier, T.E., Damke, H., Tisdale, E.J., Meyerowitz, E.M., and Schmid, S.L. 1993. Mutations in human dynamin block an intermediate stage in coated vesicle formation. J. Cell Biol. *122*, 553–563.

Warnock, D.E., Hinshaw, J.E., and Schmid, S.L. (1996). Dynamin self-assembly stimulates its GTPase activity. J. Biol. Chem. *271*, 22310–22314.

Warnock, D.E., and Schmid, S.L. (1996). Dynamin GTPase, a force generating molecular switch. BioEssays *18*, 885–893.

Warnock, D.E., Terlecky, L.J., and Schmid, S.L. (1995). Dynamin GTPase is stimulated by crosslinking through the C-terminal proline-rich domain. EMBO J. *14*, 1322–1328.